Greensphere:
Journal of Environmental Chemistry
ISSN: 2777-0664

Review Article

Comparative Review of Cellulose Acetate, Polyacrylonitrile, and Polyvinyl Alcohol-Based Hydrophilic Membranes for Desalination

Romario Abdullah[1]*, Alvin Romadhoni Putra Hidayat[2], Novia Amalia Sholeha[1]
[1]College of Vocational Studies, Bogor Agricultural University (IPB University), Bogor, Indonesia
[2]Department of Chemistry, Diponegoro University, Semarang, Indonesia
**Corresponding author*: romario@apps.ipb.ac.id

Received: 25 April 2026/ Accepted: 27 Mei 2026
Available online: 31 Mei 2026

Abstract

The issue of clean water scarcity has become one of the most critical challenges threatening the global population today. It is estimated that approximately 6 billion people will experience water stress and shortages by 2050. One promising solution to address this challenge is the implementation of desalination technologies to convert seawater into freshwater. Among the available approaches, membrane-based desalination offers significant advantages, including lower energy requirements, cost-effective fabrication, and improved environmental sustainability. Polymeric membranes with high hydrophilicity have shown considerable potential for further development, particularly those based on cellulose acetate (CA), polyacrylonitrile (PAN), and polyvinyl alcohol (PVA), each exhibiting distinct advantages as materials for desalination applications. Key parameters influencing membrane performance include hydrophilicity, permeability, membrane thickness, pore size, and porosity. Based on the reviewed studies, membranes synthesized using PVA demonstrate superior characteristics in terms of permeability, optimal thickness, pore size, and porosity. These properties contribute to enhanced water flux and salt rejection performance compared to membranes fabricated from CA and PAN.

Keywords: *Desalination; Hydrophilic; Polymeric membranes; Water treatment*

1. Introduction

The scarcity of clean water has become one of the most pressing global challenges threatening human populations today. It is estimated that approximately 6 billion people will experience water stress and shortages by 2050 [1]. Of the total freshwater available on Earth, only about 30% is accessible for daily human use, while the remaining portion is locked in glaciers and underground reserves [2]. Industrial activities are considered one of the major contributors to global water scarcity, alongside climate change and rapid population growth. These factors have significantly increased the demand for clean water in everyday life [3]. Efforts to address this issue include raising awareness and responsibility among communities and industrial stakeholders to reduce pollution caused by illegal discharge of domestic and industrial waste into water bodies. However, public awareness regarding water scarcity remains relatively low, leading to continued practices that exacerbate water pollution. Therefore, effective and sustainable solutions are urgently needed to overcome this challenge. One promising approach is to utilize advancements in science and technology, combined with the abundant availability of seawater, through chemical based methods to enhance freshwater production. One such method is desalination [4].

Desalination is one of the primary technologies widely employed to produce freshwater from seawater and other saline sources [5]. It involves the removal of dissolved salts from saline water to generate potable water. Broadly, desalination technologies can be categorized into three main approaches: membrane-based processes, distillation, and chemical reaction based methods [6]. Among these, distillation and chemical approaches are often considered complex and relatively costly. In addition, distillation methods may suffer from lower water purity levels. Consequently, membrane-based desalination has emerged as a more favorable alternative. Membrane technology has experienced rapid development in recent years due to its strategic role in separation processes [7]. Compared to conventional separation technologies, membrane systems offer several advantages, including lower energy consumption,

operational simplicity, cost-effectiveness, and environmental sustainability [8]. The application of membranes for efficient ion separation from aqueous solutions has been a central focus in membrane science over the past decades, driven by the increasing demand for affordable technologies in seawater desalination, wastewater treatment, and related applications [9]. Generally, two types of membranes are used in desalination: water permeable membranes that reject ions, and ion exchange membranes that allow ion transport but restrict water passage [10]. Various desalination membrane technologies have been extensively developed, including reverse osmosis (RO), forward osmosis (FO), pervaporation (PV), membrane distillation (MD), dialysis (DA), electrodialysis (ED), and nanofiltration (NF) [11].

Based on their composition, membranes are classified into organic (polymeric) and inorganic types. Inorganic membranes have been widely explored in desalination due to their excellent thermal stability, resistance to harsh environments, and ability to withstand high pressures [12]. However, they generally involve high production costs and exhibit relatively rigid mechanical properties. As an alternative, polymeric membranes have gained significant attention, as they not only possess favorable chemical properties and pressure resistance but also offer lower production costs compared to inorganic membranes. These advantages make polymeric membranes more effective and economically viable as base materials for desalination membrane fabrication [13]. With the advancement of polymeric membranes, increasing attention has been directed toward the design of membranes with enhanced hydrophilic properties to improve desalination performance. Hydrophilicity plays a crucial role in enhancing water affinity, facilitating faster water molecule transport, and mitigating fouling, which remains one of the primary challenges in separation processes. Therefore, the selection of polymeric materials with inherent hydrophilic characteristics has become an effective strategy for developing more efficient and sustainable desalination membranes.

Several hydrophilic polymers that have been extensively studied and developed for desalination membrane applications include cellulose acetate (CA), polyacrylonitrile (PAN), and polyvinyl alcohol (PVA). Cellulose acetate is well known for its excellent film forming ability and biodegradability, which supports sustainability aspects. Meanwhile, PAN exhibits high chemical and mechanical stability, making it suitable for operation under relatively harsh conditions. In contrast, PVA demonstrates superior hydrophilicity, ease of modification, and the ability to form membrane structures with optimal porosity. The combination of these advantageous properties positions CA, PAN, and PVA as promising candidates for the development of high-performance hydrophilic polymer-based desalination membranes [14]–[16].

This article aims to comprehensively examine the potential of highly hydrophilic polymeric materials as base components for desalination membrane fabrication, focusing on CA, PAN, and PVA. These materials represent a class of polymers that have been extensively developed and widely applied in desalination technologies, and they are expected to exhibit significant potential in addressing global water scarcity challenges. The novelty of this review lies in its specific focus on the comparative analysis of hydrophilic polymer-based desalination membranes, particularly CA, PAN, and PVA, which has not been comprehensively discussed in previous review articles. Previous review studies generally reported desalination of membranes from a broad perspective, focusing on membrane technologies, fabrication methods, or overall membrane materials without specifically emphasizing the hydrophilic characteristics of the polymers used. In contrast, this review specifically highlights the importance of polymer hydrophilicity and its relationship with desalination membrane performance. Through the comparison of key membrane properties, including permeability, pore size, membrane thickness, porosity, flux, and salt rejection, this review is expected to provide valuable insights into the potential of hydrophilic polymers for developing superior and high-performance desalination membranes for future water treatment applications.

2. Method

The literature review process employed in this study is illustrated in the PRISMA flowchart shown in Figure 1. A comprehensive literature search was conducted using the Google Scholar database to identify relevant studies related to hydrophilic polymer-based desalination membranes, particularly CA, PAN, and PVA. The search included publications from 2010 to 2026 to capture the recent progress and development trends in membrane desalination technologies. Several keyword combinations and Boolean search strings were applied, including “desalination membrane”, “cellulose acetate desalination membrane”, “polyacrylonitrile desalination membrane”, “PVA desalination membrane”, and “hydrophilic polymer membrane for desalination”. The initial search yielded 186 records. Only research articles written in English and focused on membrane desalination applications were considered for further analysis.

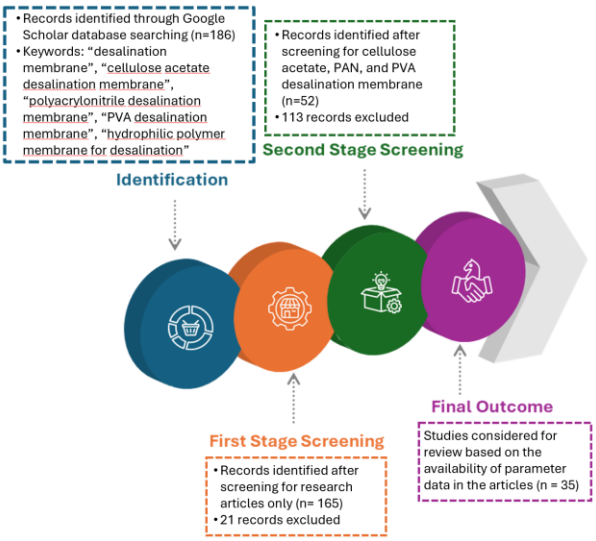

Figure 1. The PRISMA flowchart of the search and selection papers

3. Development of Desalination Membranes for Water Treatment

Membrane desalination (MD) is a relatively recent and promising technology for seawater desalination. It is particularly suitable for small to medium scale applications that require substantial water supply and can operate under atmospheric pressure and temperatures below 100°C. MD is a non isothermal separation process that has attracted significant research interest due to its relatively low operational cost [3]. The separation mechanism in this process is primarily governed by differences in component volatility, where vapor pressure gradients act as the driving force for desalination [17]. In the MD process, the heated feed solution comes into contact with a microporous membrane, enabling the transport of water molecules in vapor form across the membrane. The efficiency of this transport process is strongly influenced by membrane characteristics such as pore size, surface properties, and structural morphology. In this context, the incorporation of hydrophilic properties into membrane materials has gained increasing attention. Hydrophilic membranes enhance water affinity, facilitate water molecule adsorption at the membrane interface, and promote more efficient mass transfer. Furthermore, improved hydrophilicity can contribute to reduced fouling tendencies and enhanced operational stability, which are critical factors in long-term desalination performance. Compared to conventional distillation processes, MD offers several advantages, including a significantly higher specific surface area, which enhances process efficiency. Additionally, MD operates at relatively lower temperatures, allowing the utilization of low grade heat sources such as industrial waste heat and geothermal energy. As a thermally driven separation process, MD typically operates under relatively low pressure conditions, generally up to several hundred kPa, which is considerably lower than pressure driven membrane processes such as ultrafiltration and reverse osmosis [18]. Desalination technologies can be broadly classified into three main categories: evaporation and condensation, filtration, and crystallization, as illustrated in Figure 2.

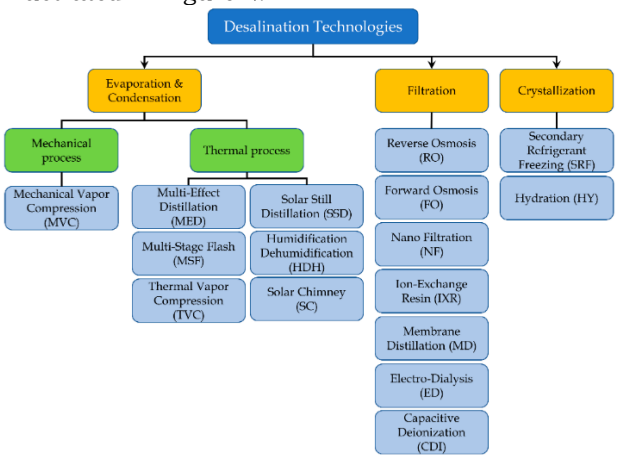

Figure 2. Classification of desalination technologies, including evaporation and condensation processes, membrane-based filtration, and crystallization [19]

In membrane distillation, separation is governed by a temperature induced vapor pressure gradient across the membrane, enabling phase change and vapor transport [7]. In contrast, reverse osmosis operates based on a hydraulic pressure gradient, where the applied pressure exceeds the osmotic pressure to drive solvent transport through a dense, non porous membrane. This distinction highlights the difference between thermally driven and pressure driven membrane processes. As illustrated in Figure 3, reverse osmosis relies on the direct transport of water molecules through a semi-permeable membrane while rejecting dissolved salts and other contaminants. The schematic representation emphasizes the role of applied pressure, pretreatment, and membrane selectivity in achieving efficient desalination. Therefore, comparing membrane distillation with reverse osmosis provides a broader understanding of the operational principles, advantages, and limitations of each technology in desalination applications [20]. Lower operating pressures lead to reduced equipment costs and enhanced process safety. On the other hand, this process is considered highly practical due to its theoretical separation efficiency of up to 100%, where all ions, macromolecules, microorganisms, and non-volatile constituents can be effectively rejected. Furthermore, membrane fouling is not regarded as a critical issue in terms of transport rate, as the pore sizes are relatively large compared to diffusion pathways, making them less susceptible to blockage [21].

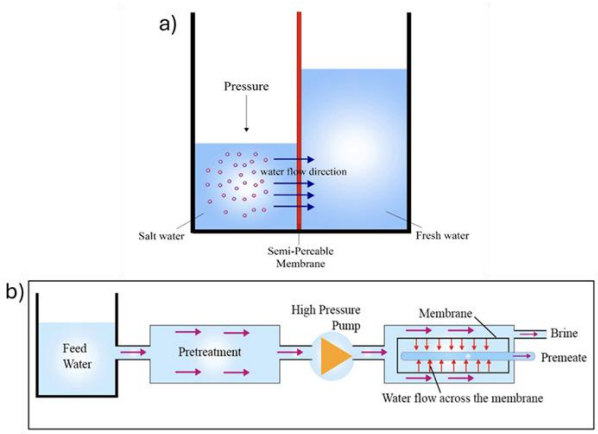

Figure 3. (a) Schematic illustration of the reverse osmosis mechanism (b) Process flow diagram of a reverse osmosis desalination system [20]

In membrane distillation, the temperature gradient across the membrane interface induces a vapor pressure difference between the components being separated, thereby generating the driving force for mass transfer [7]. The liquid on the hot side (feed side) evaporates at the membrane surface, diffuses through the membrane pores in the vapor phase, and subsequently condenses on the cold side. Separation occurs partly during vapor diffusion and partly due to vapor liquid equilibrium conditions at the membrane solution interface. Any comprehensive model for membrane distillation must account for the influence of boundary layers, transmembrane flux, vapor liquid equilibrium at the membrane interface, and temperature effects [22]. Figure 4 presents the publication trends in MD research from 2016 to 2026 based on data obtained from ScienceDirect. Figure 4a shows the total number of membrane distillation publications per year, while Figure 4b illustrates the annual publication distribution of hydrophilic polymer-based membranes, including CA, PAN, and PVA.

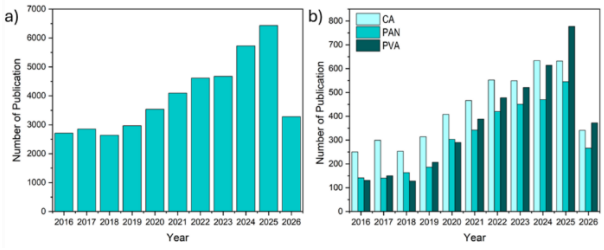

Figure 4. Publication trends in membrane distillation research from 2016 to 2026: (a) total number of publications on membrane distillation per year, and (b) annual publication output on hydrophilic polymer-based membranes

4. Hydrophilic Polymer Materials in the Fabrication of Desalination Membranes

4.1 Cellulose Acetate

Cellulose acetate (CA) is one of the most widely used hydrophilic polymers for desalination membrane fabrication due to its excellent film-forming ability, good hydrophilicity, biodegradability, and relatively low production cost [23-24]. CA membranes have been extensively applied in reverse osmosis, nanofiltration, and membrane distillation because they exhibit favorable water permeability and salt rejection performance [25]. In addition, the abundant hydroxyl and acetyl functional groups in CA contribute to improved water affinity and membrane formation characteristics [24]. CA is commonly synthesized through the acetylation of cellulose using acetic anhydride in the presence of acid catalysts, and the resulting polymer can be tailored to achieve desirable membrane structures and separation performance (Figure 5). This requirement is essential to achieve good polymer solubility, which is critical for membrane fabrication, as impurities such as hemicellulose can form undesirable gels. Cellulose acetate is widely used as a polymeric material in membrane fabrication and is also being explored for other desalination techniques such as forward osmosis and membrane distillation [23]. This polymer is a semi crystalline thermoplastic that is insoluble in water, yet highly hydrophilic due to the presence of hydroxyl (–OH) groups and acetyl groups along its polymer backbone [26-27]. Cellulose acetate can be fabricated into asymmetric membranes using a phase inversion technique, typically involving immersion in a water bath. The selection of solvent is a critical factor, as it significantly influences membrane performance through solvent nonsolvent exchange while maintaining the density of the membrane's top skin layer. Cellulose acetate demonstrates strong potential for salt rejection in seawater desalination processes and is relatively easy to process and apply [28].

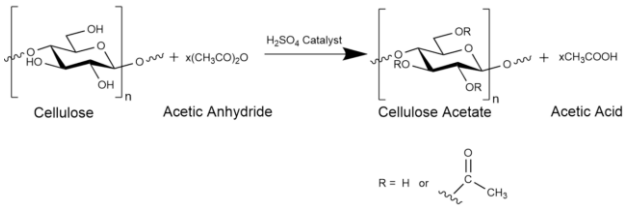

Figure 5. Synthesis of cellulose acetate via acetylation of cellulose

Chen et al. (2025) developed a nanofiltration membrane for desalination using cellulose acetate as the polymer matrix, incorporating a charge gradient structure via the surface segregation of ionic covalent organic framework nanosheets (iCOFNs). The incorporation of iCOFNs significantly enhanced both the surface charge and structural properties of the cellulose acetate membrane, as evidenced by an increase in surface charge density from −0.98 to 1.13 mC/m² and a reduction in pore size from 0.74 to 0.68 nm, thereby improving salt rejection performance. In addition, the membrane thickness decreased progressively with increasing iCOFN content, as illustrated in Figure 6a-c. The membrane performance results demonstrated that the cellulose acetate membrane embedded with iCOFNs achieved Na_2SO_4 rejection of up to 95% and maintained stable operation for up to two months with a rejection rate of approximately 95%. This enhanced performance

can be attributed to the presence of sulfonate rich iCOFNs within the CA polymer matrix, which induce a steric hindrance effect, as shown in Figure 5d. Furthermore, the sulfonate groups increase the negative surface charge density of the membrane (Figure 6e), thereby strengthening electrostatic repulsion against salt ions [29].

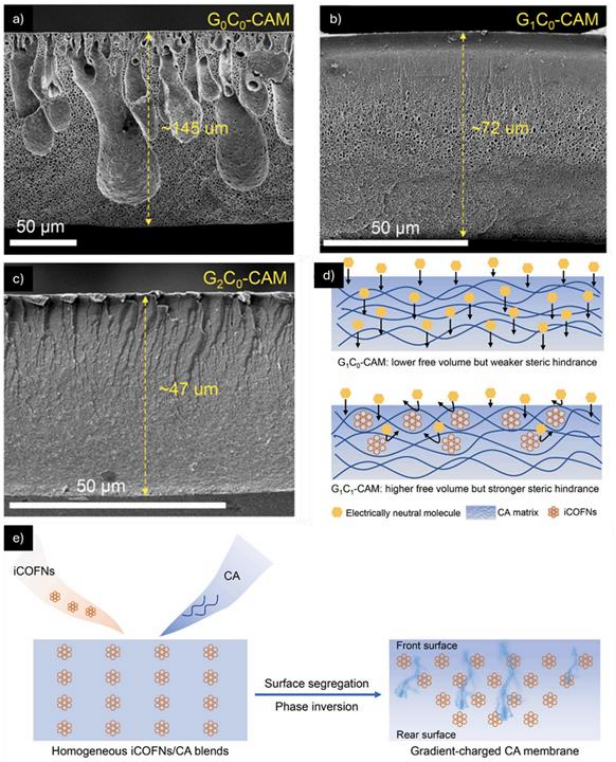

Figure 6. (a–c) SEM images of membranes with varying composition, (d) Schematical illustration of steric hindrance effect in membrane, and (e) Conceptual illustration of gradient charged cellulose acetate membrane (GC-CAM) formed by surface segregation of iCOFNs during phase inversion [29]

Similarly, Rashad et al. (2025) reported that the incorporation of hydrophilic cellulose acetate layers into dual layer composite membranes (Figure 7) enhanced desalination performance in the Direct Contact Membrane Distillation (DCMD) process. The improved membrane hydrophilicity, reflected by the reduced contact angle, promoted more efficient vapor condensation and water transport, thereby increasing the flux to 17.57 LMH while maintaining salt rejection above 99.9%. Compared with conventional hydrophobic membranes, the presence of the CA layer also improved, fouling resistance, highlighting the important role of hydrophilic polymers in mitigating membrane fouling during long-term desalination operation. These findings collectively demonstrate that enhancing membrane hydrophilicity through polymer blending or nanomaterial incorporation can effectively improve both flux and separation performance. However, despite the promising results, most studies remain limited to laboratory scale evaluations, and further investigation is still required to assess long-term mechanical stability, scalability, and membrane performance under real seawater operating conditions [30].

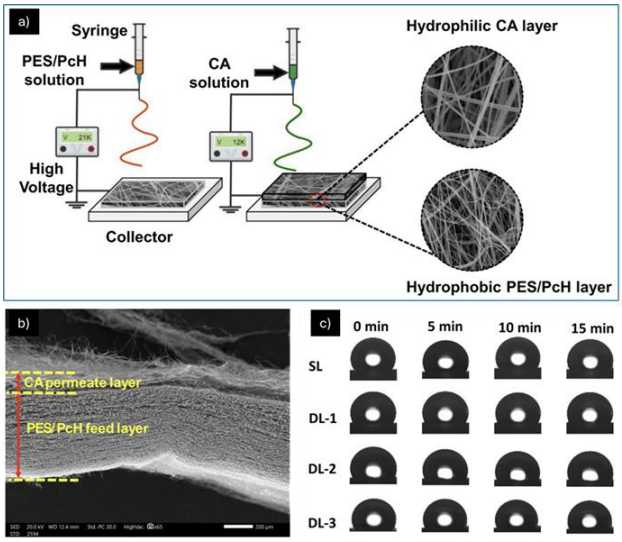

Figure 7. (a) Schematic illustration of electrospinning setup used for DL membranes fabrication, (b) SEM of PES/PcH/CA membrane and (c) Corresponding WCA images for each membrane type [30].

The desalination performance of CA-based membranes is strongly influenced by the type of blending materials, membrane morphological characteristics, and operational conditions during the filtration process. Numerous studies have demonstrated that the incorporation of materials such as graphene oxide (GO), carbon nanotubes (CNT), polyethylene glycol (PEG), AMPS, PES-PcH, iCOFNs, and various nanoparticles can significantly enhance membrane hydrophilicity, porosity, structural stability, and water transport pathways. Carbon-based nanomaterials generally contribute to improved permeability and water flux through the formation of nanochannels and increased active surface area, whereas specific polymeric blends predominantly enhance membrane selectivity and salt rejection capability. In addition, parameters including pore size, membrane thickness, operating pressure, and feed salt concentration play critical roles in determining the trade-off between permeation flux and ion rejection performance. Therefore, optimizing material composition and fabrication conditions remains a crucial aspect in the development of CA-based membranes with superior desalination performance in terms of both permeability and separation selectivity. Several previous studies related to desalination membranes based on cellulose acetate polymers are summarized in Table 1.

4.2 Polyacrylonitrile

Polyacrylonitrile (PAN) is a synthetic polymer that has been extensively explored as a membrane material for desalination and water treatment applications due to its excellent chemical resistance, thermal stability, and mechanical strength [42]. These properties enable PAN-based membranes to maintain structural integrity under relatively harsh

operating conditions, making them suitable for processes such as ultrafiltration, nanofiltration, reverse osmosis, and membrane distillation. In addition, the nitrile (–C≡N) functional groups present in the PAN backbone provide opportunities for surface modification and functionalization, which can improve membrane hydrophilicity, permeability, and antifouling characteristics [43]. As a result, PAN has become one of the most promising polymers for the fabrication of high performance desalination membranes. PAN is commonly synthesized through the polymerization of acrylonitrile monomers using various solvent systems such as N,N-dimethylformamide (DMF), dimethyl sulfoxide (DMSO), or dimethylacetamide (DMAc) [44]–[46]. The physicochemical properties of PAN membranes can be tailored through copolymerization, blending, surface treatment, and incorporation of nanomaterials to optimize membrane morphology and separation performance. Furthermore, PAN exhibits excellent compatibility with inorganic nanoparticles and carbon based nanomaterials, facilitating the development of nanocomposite membranes with enhanced water flux, salt rejection, and fouling resistance [46]. Owing to its versatile structure and stability, PAN has also been widely employed as a precursor material for advanced carbon-based membranes and hollow fiber membrane systems used in desalination technologies [47].

The use of PAN in desalination membranes has been widely established due to its excellent resistance to hydrolysis and oxidation. In addition, PAN exhibits relatively high crystallinity and inherent hydrophilic characteristics. In membrane applications, PAN is often copolymerized with other polymers to further enhance hydrophilicity and reduce material brittleness [48]. PAN membranes typically exhibit a water contact angle of approximately 46°, indicating favorable wettability that allows water to permeate efficiently while simultaneously repelling hydrophobic substances such as oils and fats. This characteristic provides a significant advantage for desalination processes. Structurally, PAN membranes display finger-like pore formations on the surface, followed by macrovoids beneath the top layer. This represents a typical asymmetric morphology formed through nonsolvent-induced phase separation techniques [49].

Mazhari et al. (2023) developed a forward osmosis membrane-based on a thin-film composite (TFC) structure using a PAN substrate modified with nitrogen-doped carbon quantum dots (BWD-NCQDs), which were synthesized from banana peel waste, as illustrated in Figure 8a. The incorporation of BWD-NCQDs was intended to enhance desalination performance by improving membrane hydrophilicity and intrinsic transport properties (Figure 8b). The improvement in membrane hydrophilicity was evidenced by a decrease in contact angle from 61.7 to 36.3° (Figure 8c), which contributed to an increase in water flux by up to 54.7 LMH and NaCl rejection of up to 96.2%. Furthermore, the membrane exhibited excellent fouling resistance, with a flux recovery ratio (FRR) of 98.8%. These improvements are mainly attributed to the formation of a more hydrophilic and negatively charged membrane surface, which not only promotes water permeation but also suppresses foulant accumulation through electrostatic repulsion mechanisms. This study highlights the potential of combining hydrophilic PAN matrices with sustainable carbon based nanomaterials to simultaneously improve permeability, selectivity, and fouling resistance in desalination membranes [50].

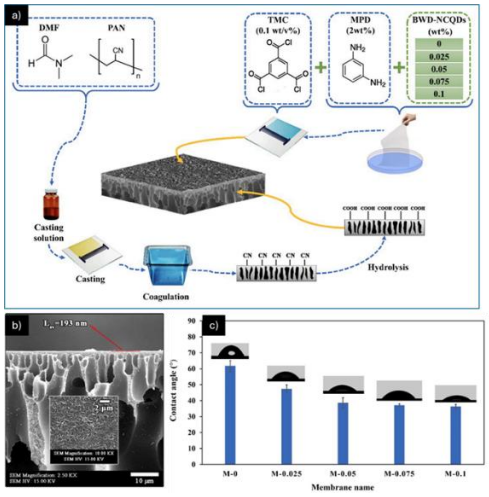

Figure 8. (a) A Flow chart of TFC-FO membrane preparation, (b) The SEM images of the TFC-FO membranes, and (c) Water contact angle of the BWD-NCQDs-incorporated and pristine FO membranes [50].

Dai et al. (2024) reported the fabrication of a nanofiltration membrane incorporating hydrolyzed polyacrylonitrile (HPAN) nanofibers, as illustrated in Figure 9a. The membrane was specifically engineered to enhance the permeability of conventional NF membranes by improving surface hydrophilicity, as shown in Figure 9b. The presence of negatively charged COO^- functional groups on HPAN facilitates the electrostatic attraction of positively charged piperazine (PIP) monomers, thereby promoting greater monomer retention within the interlayer. This effect contributes to the formation of a more efficient selective layer. The resulting membrane exhibited a water permeability of up to 33.7 LMH/bar, which is significantly higher than that of membranes without HPAN incorporation. In addition, the membrane demonstrated excellent salt rejection performance (Figure 9c), achieving rejection rates of 98.9% for Na_2SO_4 and 99.7% for $MgSO_4$. Furthermore, the membrane displayed strong mechanical stability, maintaining structural integrity under pressures up to 7 bar and sustaining stable operation for at least 20 hours of continuous testing [51].

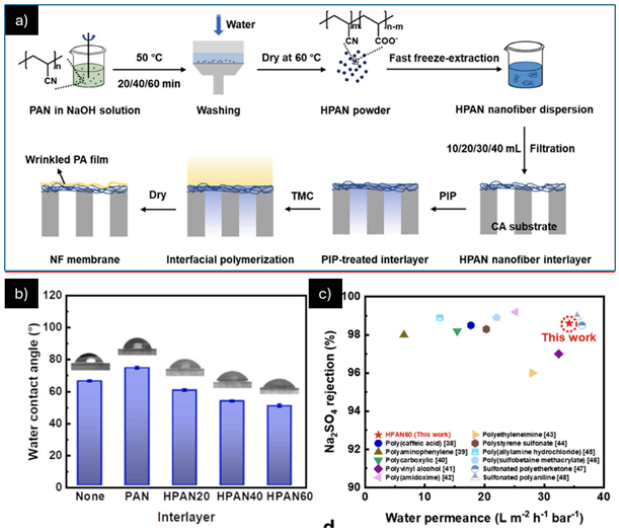

Figure 9. (a) Schematic of the fabrication of PA NF membranes with freeze-extracted HPAN nanofibers as interlayers, (b) Water contact angles, and (c) Performance of PA NF membranes [51].

Table 1. Desalination Membranes Based on Cellulose Acetate

Polymer Material	Matrix Blend Material	Process Type	Membrane Characteristics	Feed Solution	Operating Conditions (Temperature, [NaCl], Driving Force)	Flux (LMH)	Salt Rejection (%)	Reference
CA	PES-PcH	Direct Contact Membrane Destillation	Flat-sheet, Thickness: 246.6 µm, Porosity: >89%	NaCl	68 °C; 13000 ppm NaCl; vapor pressure gradient	17.57	>99.9	[30]
CA	iCOFNs	Nanofiltration	Flat-sheet; Permeability: 0.46 LMH/bar; Thickness: 47 µm; Pore size: 0.68 nm	NaCl, $MgSO_4$, $MgCl_2$, KCl, Na_2SO_4, LiCl	20 °C; 4 bar; 1000 ppm NaCl; hydrostatic pressure	-	74.6	[29]
CA	GO-PAMAM	Nanofiltration	Flat-sheet; Thickness: 100 µm; Porosity: 74%	NaCl, $MgCl_2$, Na_2SO_4	5–8 bar; 2000 ppm NaCl; pressure difference	11.26	52	[31]
CA	GO/AA/CTA	Forward Osmosis	Flat-sheet; Thickness: 200 µm; Porosity: 62%	NaCl	25 °C; 49.26 bar; 58440 ppm NaCl; osmotic-pressure gradient	33.6	99.88	[32]
CA	PVCA	Reverse Osmosis	Flat-sheet; Permeability: 2.42 LMH/bar; Thickness: 200 µm	NaCl	25 °C; 6 bar; 2000 ppm NaCl; hydrostatic pressure	14.53	99.56	[33]
CA	AMPS	Reverse Osmosis	Flat-sheet; Thickness: 250 µm	NaCl	25 °C; 4 bar; 10000 ppm NaCl; pressure difference	17.11	99.24	[34]
CA	PEG	Reverse Osmosis	Flat-sheet; Pore size: 0.1–1 nm	NaCl	25 °C; 55.16 bar; 2000 ppm NaCl; pressure difference	1.36	95.4	[35]
CA	GO	Reverse Osmosis	Flat-sheet; Thickness: 100 µm; Pore size: 6 nm	NaCl	25 °C; 25 bar; 25000 ppm NaCl; hydrostatic pressure	65	90	[36]
CA	-	Reverse Osmosis	Flat-sheet; Permeability: 0.5 LMH/bar; Thickness: 0.217 µm	NaCl	26 °C; 30 bar; 2000 ppm NaCl; hydrostatic pressure	18	68	[37]
CA	CNT	Reverse Osmosis	Flat-sheet; Thickness: 7 µm; Pore size: 140 nm	NaCl	25 °C; 30 bar; 5000 ppm NaCl; pressure difference	130	96	[38]
CA	GO	Reverse Osmosis	Flat-sheet; Thickness: 0.04 µm; Pore size: 0.9 nm; Porosity: 129%	NaCl	25 °C; 30 bar; 2000 ppm NaCl; pressure difference	13.65	82.03	[39]
CA	CNT	-	Flat-sheet; Thickness: 100 µm; Pore size: 117 nm	NaCl	25 °C; 24 bar; 1000 ppm NaCl; pressure difference	18	68.8	[40]

Polymer Material	Matrix Blend Material	Process Type	Membrane Characteristics	Feed Solution	Operating Conditions (Temperature, [NaCl], Driving Force)	Flux (LMH)	Salt Rejection (%)	Reference
CA	PEG	-	Flat-sheet; Thickness: 250 µm; Porosity: 75%	NaCl	25 °C; 20 bar; 2000 ppm NaCl; pressure difference	41.5	93	[14]
CA	ZNPs	Reverse Osmosis	Flat-sheet; Thickness: 250 µm	NaCl	25 °C; 10 bar; 10000 ppm NaCl; hydrostatic pressure	1.78	86.8	[41]

The reviewed studies demonstrated that PAN-based desalination membranes (Table 2) exhibit outstanding salt rejection performance, generally exceeding 96%, highlighting the significant potential of PAN as a hydrophilic polymer matrix for desalination applications. Among the reported systems, PAN/PVDF membranes achieved the highest salt rejection value of 99.99% while maintaining a relatively high water flux of 83.4 LMH, indicating that blending PAN with hydrophobic polymers such as PVDF can substantially enhance separation efficiency without compromising water productivity. Similarly, PAN membranes modified with GO and PVDF/NMP also exhibited rejection values above 99.8%, emphasizing the crucial role of nanomaterial incorporation and polymer blending in improving membrane selectivity and structural stability. Nevertheless, despite the excellent rejection performance, several studies reported relatively low operating pressures, particularly in membrane distillation systems, suggesting that membrane morphology and transport mechanisms strongly influence desalination performance beyond the intrinsic properties of the polymer itself. Interestingly, membranes with larger pore sizes and higher porosity did not consistently demonstrate superior flux performance, indicating that factors such as surface hydrophilicity, interfacial compatibility, and membrane compactness also play essential roles in transport efficiency. Therefore, future investigations should focus on the standardization of testing conditions and the provision of more comprehensive membrane characterization data to enable more reliable performance comparisons and a deeper understanding of the operational mechanisms governing hydrophilic polymer-based desalination membranes.

4.3 Polyvinyl Alcohol

Polyvinyl alcohol (PVA) is a synthetic hydrophilic polymer that has attracted considerable attention in desalination membrane development due to its high water affinity, excellent film forming capability, and flexible chemical structure [56]. The presence of abundant hydroxyl (–OH) groups within the polymer chains promotes strong interactions with water molecules, thereby enhancing membrane wettability and water transport properties [57]. These characteristics make PVA highly suitable for various desalination processes, including membrane distillation, pervaporation, nanofiltration, and reverse osmosis applications. In addition, PVA exhibits good compatibility with various nanomaterials and crosslinking agents, enabling further improvement of membrane selectivity, permeability, and antifouling performance [58], [59]. PVA is commonly synthesized through the hydrolysis of poly(vinyl acetate) (PVAc), in which acetate groups are converted into hydroxyl groups under acidic or alkaline conditions [60]. The degree of hydrolysis and polymerization significantly influences the physicochemical properties of PVA, including solubility, mechanical stability, crystallinity, and hydrophilicity [61]. Highly hydrolyzed PVA generally demonstrates stronger intermolecular hydrogen bonding, resulting in enhanced structural integrity and improved membrane stability during desalination operations. Furthermore, the tunable structure of PVA facilitates membrane modification through blending, crosslinking, and nanocomposite formation, which are widely employed strategies to optimize desalination membrane performance in terms of flux, salt rejection, and fouling resistance.

Saad et al. (2024) reported a study on the synthesis and characterization of desalination membranes fabricated from a blend of sodium alginate and PVA, with epichlorohydrin employed as a crosslinking agent. Scanning Electron Microscopy (SEM) analysis revealed that the membrane possessed an average pore size of approximately 42 µm and a compressive strength of 20.67 kN/m². The desalination performance demonstrated a water flux of up to 0.845 LMH [62]. Liu et al. (2026) developed a chitosan based desalination membrane modified with the incorporation of PVA (Figure 10a). Schematic of the solar driven evaporation setup using a xenon lamp, equipped with a hygrometer, electronic balance, and IR camera for monitoring, shown in Figure 10b) The membrane characterization indicated that the addition of PVA significantly enhanced the tensile strength from 4.5 to 7.5 MPa and increased elongation at break to 23.7%. Furthermore, the hydrophilic nature of PVA improved the membrane's surface hydrophilicity, as evidenced by a reduction in contact angle to 42.96°, and increased the swelling degree to 142.06%, attributed to the abundance of hydroxyl functional groups. The membrane performance also exhibited a water flux of 6.762 L/m²·h with a salt rejection of up to 98.8%. Schematic of the solar driven evaporation setup using a xenon lamp, equipped with a hygrometer, electronic balance, and IR camera for monitoring. Water production over five days, showing relatively stable performance with a slight decrease on later days due to environmental conditions (Figure 10c). These findings highlight the considerable potential of PVA in desalination membrane applications [63].

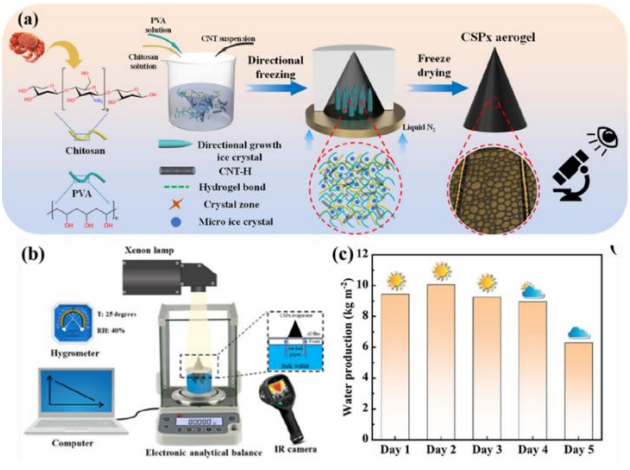

Figure 10. (a) The preparation process of the CSPx aerogel, (b) Schematic diagram of the solar steam power performance assessment, and (c) The water production of continues five days [63]

PVA-based desalination membranes have demonstrated remarkable desalination performance (Table 3), particularly in achieving consistently high salt rejection values approaching 100%, which can be strongly associated with the superior hydrophilic nature of PVA compared to many conventional polymeric membrane materials. The abundant hydroxyl functional groups present in PVA contribute to enhanced water affinity, facilitating rapid water transport while maintaining effective salt exclusion. The incorporation of functional additives and blending materials such as silica, CNT, SNC, PVDF, and stilbazol further improved membrane permeability, structural stability, and flux performance without significantly compromising selectivity. Among the reported studies, the PVA/stilbazol membrane exhibited the highest flux value of 122.6 LMH, whereas PVA/CA and PVA/PVDF membranes achieved outstanding salt rejection values of 99.99%, indicating that chemical modification and interfacial engineering effectively optimize membrane transport properties. Nevertheless, the substantial variation in membrane thickness, pore size, operating pressure, salinity concentration, and temperature among the studies suggests that membrane performance is highly influenced by experimental conditions and fabrication parameters. Therefore, despite the promising potential of PVA-based membranes as highly hydrophilic desalination materials, more standardized testing protocols and comprehensive characterization are still required to establish clearer correlations between hydrophilicity, membrane morphology, and desalination efficiency.

Table 2. Desalination Membranes Based on Polyacrylonitrile

Polymer Material	Matrix Blend Material	Process Type	Membrane Characteristics	Feed Solution	Operating Conditions (Temperature, [NaCl], Driving Force)	Flux (LMH)	Salt Rejection (%)	Reference
PAN	BWD-NCQDs	Forward Osmosis	Thin Film Composite; Permeability: 3.17 LMH/bar; Thickness: 100 μm	NaCl	Temperature: 25 °C; Pressure: 3 bar; NaCl: 35064 ppm; osmotic-pressure	54.7	96.2	[50]
PAN	-	Pervaporation	Flat-sheet; Thickness: 149 μm; Pore size: 5.2 nm; Porosity: 68%	NaCl	Temperature: 25 °C; Pressure: 0.004 bar; NaCl: 100000 ppm; Partial vapor pressure difference	82	99.93	[15]
PAN	PVA	Pervaporation	Thin Film Nanofibrous; Thickness: 12.9 μm; Pore size: 275 nm	NaCl	Temperature: 25 °C; Pressure: 0.001 bar; NaCl: 5000 ppm; Partial vapor pressure difference	8.53	99.80	[52]
PAN	GO	Pervaporation	Flat sheet; Thickness: 1.4 μm	Seawater and Brackish water	Temperature: 90 °C; Pressure: 0.001 bar; NaCl: 100000 ppm; chemical potential gradient	65	99.80	[53]
PAN	PVDF/MWNT	Direct contact membrane distillation	Thickness: 227 μm; Pore size: 0.41 μm; Porosity: 80%	NaCl	Temperature: 50.9-80.4 °C; Pressure: 1.013 bar; NaCl: 35000 ppm; pressure difference	66.9	99.80	[54]
PAN	PVDF	Direct contact membrane distillation	Hollow fiber; Permeability: 1.42 × 10^{-5} cm^2/s; Thickness: 142 μm; Pore size: 260 nm; Porosity: 83.40%	NaCl	Temperature: 60 °C; NaCl: 240000 ppm; trans-membrane vapor pressure gradient	13.30	99.10	[47]
PAN	PVDF	Direct contact membrane distillation	Hollow fiber; Thickness: 123 μm; Pore size: 480 nm; Porosity: 78.40%	NaCl	Temperature: 80 °C; NaCl: 35000 ppm; water vapor pressure gradient	83.4	99.99	[55]

Table 3. Desalination Membranes Based on Polyvinyl alcohol

Polymer Material	Matrix Blend Material	Process Type	Membrane Characteristics	Feed Solution	Operating Conditions (Temperature, [NaCl], Driving Force)	Flux (LMH)	Salt Rejection (%)	Reference
PVA	CS	Solar-driven interfacial evaporation	Aerogel 3D; Pore size: 150 nm	NaCl and Seawater	Temperature: 75 °C; NaCl: 50000 ppm; capillary pumping effect	6.762	98.8	[63]
PVA	GS	Pervaporation	Flat sheet; Pore size: 440 nm	Seawater	Temperature: 60 °C; Pressure: 0.015 bar; NaCl: 50000 ppm; chemical potential gradient	10.6	99.9	[64]
PVA	SNC	Pervaporation	Flat sheet; Thickness: 160 µm	NaCl	Temperature: 70 °C; Pressure: 0.008 bar; NaCl: 50000 ppm; water vapor pressure gradient	37.2	99.96	[65]
PVA	GA/Laponite	Pervaporation	Flat sheet; Permeability: 0.384 LMH/bar; Thickness: 160 µm	NaCl	Temperature: 70 °C; Pressure: 0.008 bar; NaCl: 30000 ppm; vapor pressure difference	58.6	99.9	[16]
PVA	CA	Reverse osmosis	Flat sheet; Permeability: 0.93 LMH/bar	NaCl and Seawater	Temperature: 25 °C; Pressure: 40 bar; NaCl: 5120 ppm; applied pressure gradient	32	99.99	[66]
PVA	-	Pervaporation	Flat sheet; Permeability: 386 LMH/bar; Thickness: 100 µm	NaCl	Temperature: 75 °C; Pressure: 0.004 bar; NaCl: 35000 ppm; chemical potential gradient	3.86	99.91	[67]
PVA	CNT	Pervaporation	Flat sheet; Permeability: 0.5 LMH/bar; Thickness: 19 µm; Pore size: 5 nm	NaCl	Temperature: 22 °C; Pressure: 0.008 bar; NaCl: 35000 ppm; vapor pressure difference	6.96	99.91	[68]
PVA	Silica	Pervaporation	Hollow fiber; Permeability: 2.29 LMH/bar; Thickness: 0.22 µm	NaCl	Temperature: 60 °C; NaCl: 2000 ppm; vapor pressure gradient	20.6	99.9	[69]
PVA	4-Sulfonylphthalic	Pervaporation	Flat sheet; Permeability: 68.1 LMH/bar; Thickness: 1.12 µm; Pore size: 66.9 nm; Porosity: 8.62%	Acid-base wastewater	Temperature: 70 °C; Pressure: 0.001 bar; NaCl: 35000 ppm; chemical potential difference	60.8	99.8	[70]

Polymer Material	Matrix Blend Material	Process Type	Membrane Characteristics	Feed Solution	Operating Conditions (Temperature, [NaCl], Driving Force)	Flux (LMH)	Salt Rejection (%)	Reference
PVA	Sulfosuccinic	Pervaporation	Flat sheet; Permeability: 137 LMH/bar; Thickness: 4.9 µm	NaCl	Temperature: 70 °C; Pressure: 0.001 bar; NaCl: 35000 ppm; chemical potential difference	27.9	99.8	[71]
PVA	Silica	Pervaporation	Flat sheet; Permeability: 369 LMH/bar; Thickness: 30 µm; Pore size: 2000 nm	NaCl	Temperature: 60 °C; Pressure: 0.01 bar; NaCl: 35000 ppm; partial vapor pressure	12.3	99.9	[72]
PVA	Stilbazol	Pervaporation	Thin-film composite; Permeability: 97 LMH/bar; Thickness: 0.2 µm; Pore size: 14 nm; Porosity: 41.40%	NaCl	Temperature: 75 °C; Pressure: 0.001 bar; NaCl: 35000 ppm; pressure gradient	122.6	99.9	[73]
PVA	Sodium periodate	Pervaporation	Flat sheet; Permeability: 68 LMH/bar; Thickness: 2 µm	NaCl	Temperature: 70 °C; NaCl: 35000 ppm; transmembrane pressure difference	34	99.93	[74]
PVA	PVDF	Pervaporation	Hollow fiber; Thickness: 2 µm; Pore size: 200 nm	NaCl, $MgCl_2$, $CaCl_2$, Na_2SO_4, $NaHCO_3$	Temperature: 80 °C; Pressure: 0.95 bar; NaCl: 100000 ppm; vapor pressure difference	16.38	99.99	[75]

5. Parameters in Desalination Membranes

5.1 Permeability

Membrane permeability is a measure that describes the rate at which a particular species penetrates through a membrane. The parameter commonly used to express permeability is flux, which is defined as the volume of permeate passing through the membrane per unit membrane area per unit time. This membrane characteristic ensures that a significant amount of water vapor can pass through the membrane within a given time. Theoretically, a high molar flux can be achieved with larger pore sizes and higher porosity, in contrast to smaller pore sizes and thicker membranes [76].

A narrow pore size distribution is also desirable, along with high porosity, as it provides a large total surface area for evaporation and water vapor transport. Meanwhile, thinner membranes result in lower mass transfer resistance for vapor transport [73]. However, in desalination membrane applications, larger pore sizes and thinner membranes do not always translate into higher molar flux. Larger pores and thinner membranes can sometimes lead to lower flux and increased conductive heat loss, which in turn reduces overall flux. Therefore, an ideal membrane should possess an optimal pore size and thickness, along with high porosity, to maximize effective mass transfer while maintaining a balance between flux and permeability. When comparing three materials cellulose acetate, polyacrylonitrile, and polyvinyl alcohol the relationship between permeability, flux, and salt rejection in desalination processes can be observed as illustrated in Figure 11. Based on the comparative analysis of the three polymers CA, PAN, and PVA generally exhibit superior permeability accompanied by relatively high-water flux, albeit with a broader variation in salt rejection performance. In contrast, CA demonstrates a more balanced trade-off between flux and salt rejection, though at comparatively lower permeability. Meanwhile, PAN shows more limited performance, characterized by lower flux and permeability. Overall, PVA stands out in terms of permeability enhancement, whereas CA offers more consistent performance in maintaining an optimal balance between flux and salt rejection, depending on the specific requirements of desalination applications.

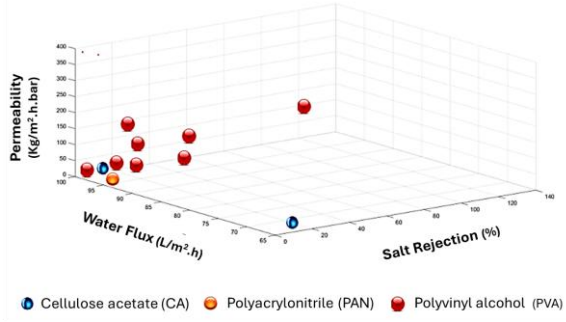

Figure 11. Comparison of permeability, flux, and salt rejection in desalination membranes

5.2 Thickness

Membrane thickness measurement is highly useful in evaluating the outcomes of the membrane synthesis process, as it serves as an indicator of uniformity and quality control. Membrane thickness can be measured using a micrometer. Theoretically, an increase in membrane thickness leads to a decrease in desalination flux [77]. The comparison of membrane thickness, water flux, and salt rejection for CA, PAN, and PVA is presented in Figure 12. The figure shows the distribution of membrane performance in terms of thickness, water flux, and salt rejection. Overall, CA membranes tend to exhibit higher thickness values with moderate water flux and relatively low to moderate salt rejection. PAN membranes show moderate thickness with stable water flux and consistent salt rejection, indicating a balanced performance. In contrast, PVA membranes display a wider variation, with several data points at lower thickness but relatively high salt rejection, although often accompanied by fluctuating water flux. This suggests that PVA can achieve good selectivity at varying structural conditions. Overall, the data highlights the trade-off among the three polymers, where CA emphasizes structural robustness, PAN offers balanced characteristics, and PVA provides higher selectivity with greater variability.

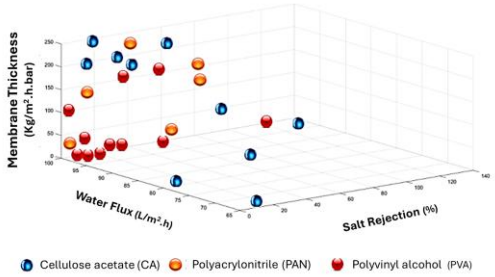

Figure 12. Comparison of membrane thickness, flux, and salt rejection in desalination membranes

5.3 Pore Size

Pore size significantly influences membrane resistance; as pore size increases, membrane resistance decreases, resulting in higher flux. A lower total resistance leads to a higher flux rate, as total resistance is inversely proportional to flux. This indicates that flux is directly proportional to membrane pore size [78]. However, to achieve optimal flux and salt rejection performance, an appropriate pore size must be selected the target species to be separated. The comparison between pore size, flux, and salt rejection for cellulose acetate, polyacrylonitrile, and polyvinyl alcohol is illustrated in Figure 13. The data indicates that CA membranes are generally associated with smaller pore sizes, accompanied by moderate water flux and relatively low salt rejection. PAN membranes exhibit intermediate pore sizes with stable water flux and more consistent salt rejection, reflecting a balanced performance. In contrast, PVA membranes show a broader distribution, including larger pore sizes and higher permeability values, with some data points achieving higher salt rejection. However, this performance is less uniform compared to the other polymers. Overall, the results suggest that pore size significantly influences membrane performance, where CA tends to favor tighter structures, PAN provides moderate characteristics, and PVA

offers more variable behavior with the potential for enhanced selectivity.

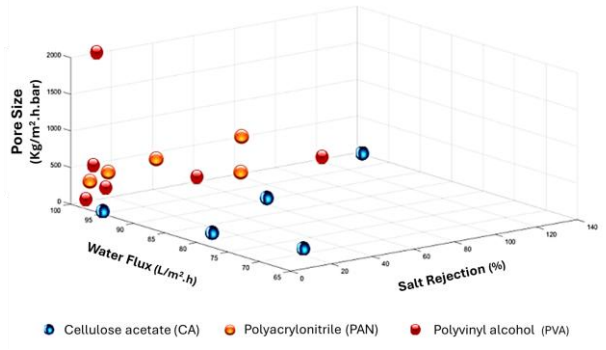

Figure 13. Comparison of membrane pore size, flux, and salt rejection in desalination membranes

5.4 Porosity

Porosity is a measure of the void spaces within a membrane material and represents the fraction of pore volume relative to the total membrane volume. Membrane porosity can be determined by calculating the rasio of pore volume to the overall membrane volume [79]. Membrane porosity refers to the volumetric fraction of empty spaces within the membrane; higher porosity provides a larger evaporation surface area. In general, membranes with higher porosity exhibit higher permeate flux and lower heat loss. The comparison between porosity, flux, and salt rejection for cellulose acetate, polyacrylonitrile, and polyvinyl alcohol is presented in Figure 14. The results show that CA membranes generally exhibit moderate porosity with relatively stable water flux and low to moderate salt rejection. PAN membranes tend to have slightly higher porosity, accompanied by high water flux and consistent salt rejection, indicating a balanced performance. Meanwhile, PVA membranes display more scattered behavior, with varying porosity and salt rejection values, although some data points indicate improved selectivity. Overall, the data suggest that porosity plays a crucial role in determining membrane performance, where CA provides stable characteristics, PAN offers a balance between permeability and selectivity, and PVA shows greater variability with potential for enhanced separation performance.

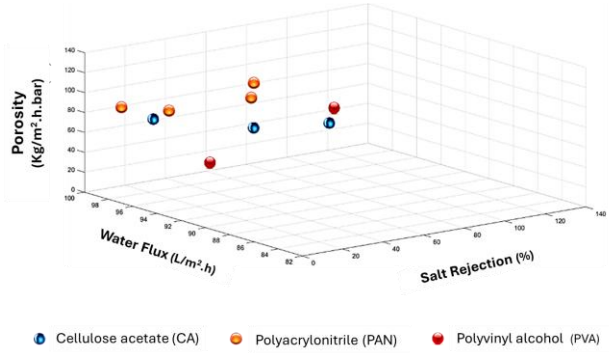

Figure 14. Comparison of membrane porosity, flux, and salt rejection in desalination membranes

6. Challenges and Future Perspectives

The permeability–selectivity trade-off should be critically considered when evaluating desalination membrane performance. Although high water flux is frequently reported as an indicator of improved membrane efficiency, elevated permeability alone does not necessarily reflect superior desalination capability if accompanied by reduced salt rejection. Several studies demonstrated that membranes with extremely high flux values often exhibited compromised ion selectivity due to enlarged pore structures or excessive membrane porosity, which may facilitate undesired salt transport. Conversely, membranes with excellent salt rejection commonly exhibited lower permeability as a consequence of denser selective layers that restrict water transport. This phenomenon indicates that achieving an optimal balance between permeability and selectivity remains one of the major challenges in the development of high-performance desalination membranes. In addition to permeability and salt rejection, long-term operational stability, fouling resistance, and energy consumption must also be considered to provide a more comprehensive assessment of membrane performance. In many reported studies, membrane evaluation was primarily conducted under short-term laboratory conditions, while limited attention was given to membrane durability, structural degradation, and fouling behavior during prolonged operation. Moreover, membranes operating at high pressure or requiring elevated thermal energy may exhibit excellent separation performance but become economically unfavorable for large-scale desalination applications. Therefore, future studies should emphasize integrated performance evaluation involving permeability, selectivity, stability, antifouling properties, and energy efficiency while simultaneously focusing on the rational selection and design of membrane materials to achieve balanced multifunctional properties that support sustainable long-term desalination performance rather than solely maximizing water flux.

7. Conclusion

Hydrophilic polymeric membranes, especially cellulose acetate (CA), polyacrylonitrile (PAN), and polyvinyl alcohol (PVA), have demonstrated considerable potential for desalination applications owing to their favorable physicochemical properties and separation performance. This review highlights that membrane performance is strongly influenced by parameters including hydrophilicity, permeability, membrane thickness, pore size, porosity, operating conditions, and membrane fabrication methods. Among the reviewed materials, PVA-based membranes generally exhibited relatively high hydrophilicity and promising desalination performance in several studies, particularly in terms of water permeability and salt rejection. However, the reported performances varied significantly depending on membrane composition, additives, modification

strategies, desalination process type, and testing conditions, making direct comparison among different studies challenging. Furthermore, this review indicates that membrane efficiency cannot be evaluated solely based on high water flux, as the permeability–selectivity trade-off, long-term operational stability, fouling resistance, mechanical durability, and energy consumption also play critical roles in determining practical desalination applicability. Several limitations remain regarding the lack of standardized testing protocols and incomplete membrane characterization across the reviewed studies. Therefore, future investigations should focus on optimizing membrane structure–property relationships, improving antifouling and mechanical stability, and developing more sustainable, energy-efficient, and cost-effective membrane fabrication strategies. In addition, rational material selection and advanced membrane design should aim to achieve balanced multifunctional properties that support long-term desalination performance and facilitate large-scale industrial implementation.

Acknowledgement

References

[1] Boretti A., dan Rosa L., 2019, Reassessing the Projections of the World Water Development Report, NPJ Clean Water, 2,1,1-6.

[2] Sarah R., Tabassum B., Idrees N., Hashem A., dan Abd_Allah E.F., 2019, Bioaccumulation of Heavy Metals in Channa punctatus (Bloch) in River Ramganga (UP), India, Saudi Journal of Biological Sciences, 26,5,979-984.

[3] Sinha Ray S. et al., 2020, RecentDevelopments in Nanomaterials-Modified Membranes for Improved Membrane Distillation Performance, Membranes, 10,7,140.

[4] Jones E., Qadir M., van Vliet M.T.H., Smakhtin V., dan Kang S., 2019, The State of Desalination and Brine Production: A Global Outlook, Science of the Total Environment, 657,1343-1356.

[5] Alkhalidi A., Kiwan S., dan Al-Hayajneh A., 2021, Experimental Investigation of Water Desalination Using Freezing Technology, Case Studies in Thermal Engineering, 28,101685.

[6] Khan M., dan Al-Ghouti M.A., 2021, DPSIR Framework and Sustainable Approaches of Brine Management from Seawater Desalination Plants in Qatar, Journal of Cleaner Production, 319,128485.

[7] Chen W., Gu Z., Ran G., dan Li Q., 2021, Application of Membrane Separation Technology in the Treatment of Leachate in China: A Review, Waste Management, 121,127-140.

[8] Rani S.L.S., dan Kumar R.V., 2021, Insights on Applications of Low-Cost Ceramic Membranes in Wastewater Treatment: A Mini-Review, Case Studies in Chemical and Environmental Engineering, 4,100149.

[9] Taghizadeh M. et al., 2021, Deep Eutectic Solvents in Membrane Science and Technology: Fundamental, Preparation, Application, and Future Perspective, Separation and Purification Technology, 258,118015.

[10] Wenten I.G. et al., 2020, Novel Ionic Separation Mechanisms in Electrically Driven Membrane Processes, Advances in Colloid and Interface Science, https://doi.org/10.1016/j.cis.2020.102269.

[11] Baysan U. et al., 2020, Frequently Used Membrane Processing Techniques for Food Manufacturing Industries, CRC Press.

[12] Kayvani Fard A. et al., 2018, Inorganic Membranes: Preparation and Application for Water Treatment and Desalination, Materials, 11,1,74.

[13] Castro-Muñoz R., 2020, Breakthroughs on Tailoring Pervaporation Membranes for Water Desalination: A Review, Water Research, https://doi.org/10.1016/j.watres.2020.116428.

[14] Abdelhamid A.E., dan Khalil A.M., 2019, Polymeric Membranes Based on Cellulose Acetate Loaded with Candle Soot Nanoparticles for Water Desalination, Journal of Macromolecular Science Part A, 56,2,153-161, https://doi.org/10.1080/10601325.2018.1559698.

[15] Fareed H. et al., 2022, Brine Desalination via Pervaporation Using Kaolin-Intercalated Hydrolyzed Polyacrylonitrile Membranes, Separation and Purification Technology, 281,119874, https://doi.org/10.1016/j.seppur.2021.119874.

[16] Selim A. et al., 2019, Preparation and Characterization of PVA/GA/Laponite Membranes to Enhance Pervaporation Desalination Performance, Separation and Purification Technology, 221,201-210, https://doi.org/10.1016/j.seppur.2019.03.084.

[17] She Q.M. et al., 2021, Layered Double Hydroxide Uniformly Coated on Mesoporous Silica, Applied Clay Science, 210,106135, https://doi.org/10.1016/j.clay.2021.106135.

[18] Abdel-Karim A. et al., 2021, Membrane Cleaning and Pretreatments in Membrane Distillation: A Review, Chemical Engineering Journal, https://doi.org/10.1016/j.cej.2021.129696.

[19] Curto D. et al., 2021, A Review of the Water Desalination Technologies.

[20] Tayeh Y.A., 2024, A Comprehensive Review of Reverse Osmosis Desalination, Desalination

and Water Treatment, 320,100882, https://doi.org/10.1016/j.dwt.2024.100882.

[21] Sathish T. et al., 2020, Multiply of Process Speed, Quality and Safety through Low-Cost Automation, AIP Conference Proceedings, 2283,20067.

[22] Cabezas R. et al., 2020, Extraction of Vanillin from Aqueous Matrices by Membrane-Based Supercritical Fluid Extraction, Industrial & Engineering Chemistry Research, 59,31,14064-14074.

[23] Islam M.D. et al., 2023, Cellulose Acetate-Based Membrane for Wastewater Treatment, Materials Advances, 4,18,4054-4102.

[24] Abu-Zurayk R. et al., 2023, Cellulose Acetate Membranes: Fouling Types and Antifouling Strategies, Processes, 11,2,489.

[25] Yang Z. et al., 2019, A Review on Reverse Osmosis and Nanofiltration Membranes for Water Purification, Polymers, 11,8,1252.

[26] Sarkar M. et al., 2023, Cellulose-Based Biodegradable Polymers: Synthesis, Properties, and Applications, Springer.

[27] Zhou X. et al., 2023, Cellulose-Based Polymers, Physical Sciences Reviews, 8,9,2001-2048.

[28] Ghaseminezhad S.M. et al., 2019, Development of Graphene Oxide-Cellulose Acetate Nanocomposite Reverse Osmosis Membrane, Composites Part B, 161,320-327.

[29] Chen R. et al., 2025, Gradient-Charged Cellulose Acetate Membranes Enabled by Ionic COF Nanosheets, Journal of Membrane Science, 734,124391, https://doi.org/10.1016/j.memsci.2025.124391.

[30] Rashad N. et al., 2025, Cellulose Acetate-Based Dual-Layer Nanofibrous Composite Membranes for Desalination, International Journal of Biological Macromolecules, 323,147186, https://doi.org/10.1016/j.ijbiomac.2025.147186.

[31] Heidari Y. et al., 2023, Improvement of Salt Rejection Efficiency of Cellulose Acetate Membrane, Heliyon, 9,9.

[32] Ahmed D.F. et al., 2021, Graphene Oxide Incorporated Cellulose Acetate Membranes, Arabian Journal of Chemistry, 14,3,102995, https://doi.org/10.1016/j.arabjc.2021.102995.

[33] Jamshaid F. et al., 2020, Synthesis and Desalination Study of Composite Membranes Integrated with Zeolites, Microporous and Mesoporous Materials, 309,110579, https://doi.org/10.1016/j.micromeso.2020.110579.

[34] Shaban M. et al., 2020, Anti-Biofouling of Grafted Cellulose Acetate Membranes for Water Desalination, Chemical Engineering Process, 149,107857, https://doi.org/10.1016/j.cep.2020.107857.

[35] Shafiq M. et al., 2018, Cellulose Acetate Thin Film Nanocomposite Membrane with TiO2 Nanoparticles, Carbohydrate Polymers, 186,367-376, https://doi.org/10.1016/j.carbpol.2018.01.070.

[36] Ghaseminezhad S.M. et al., 2019, Graphene Oxide-Cellulose Acetate Nanocomposite Membrane, Composites Part B, https://doi.org/10.1016/j.compositesb.2018.10.079.

[37] Perera D.H.N. et al., 2014, Thin Film Composite Reverse Osmosis Membranes from Cellulose Acetate, Journal of Membrane Science, 453,212-220, https://doi.org/10.1016/j.memsci.2013.10.062.

[38] El-Din L.A.N. et al., 2015, Evaluation of Cellulose Acetate Membrane with Carbon Nanotubes, Journal of Industrial and Engineering Chemistry, 26,259-264, https://doi.org/10.1016/j.jiec.2014.11.037.

[39] Shi Y. et al., 2017, Graphene Oxide–Cellulose Acetate Nanocomposite Membrane for Desalination, Journal of Materials Science, 52,13296-13306, https://doi.org/10.1007/s10853-017-1403-0.

[40] El Badawi N. et al., 2014, Carbon Nanotube-Cellulose Acetate Nanocomposite Membranes, Desalination, 344,79-85, https://doi.org/10.1016/j.desal.2014.03.005.

[41] Ali A.S.M. et al., 2021, Mixed Matrix Membranes Based on Zeolite Nanoparticles and Cellulose Acetate, Cellulose, 28,6417-6426, https://doi.org/10.1007/s10570-021-03924-5.

[42] Vatanpour V. et al., 2023, Polyacrylonitrile in Membrane Preparation, Industrial & Engineering Chemistry Research, 62,17,6537-6558.

[43] Sruthi P.R., dan Anas S., 2020, Synthetic Modification of Nitrile Group in Polymers, Journal of Polymer Science, 58,8,1039-1061.

[44] Zhang Z. et al., 2022, Pervaporation Separation Using PVA Membranes, Process Safety and Environmental Protection, 159,779-794.

[45] Niknejad A.S. et al., 2023, PAN/SAN Nanofibrous Membrane for Saline Oily Water Treatment, Desalination, 566,116895.

[46] Liu Q. et al., 2020, PAN/TiO2 Mixed Matrix Membrane, Chemical Engineering Science, 228,115993.

[47] Edwie F., dan Chung T.S., 2012, Hollow Fiber Membranes for Brine Recovery, Journal of Membrane Science, 421-422,111-123.

[48] Liang Z. et al., 2019, Electrospun Nanofiber for Lithium-Ion Batteries, Energies, 12,17.

[49] Tabe S., 2014, Electrospun Nanofiber Membranes for Water Treatment, Springer.

[50] Mazhari R. et al., 2023, Modification of PAN Membrane for Desalination, Desalination, 565,116888, https://doi.org/10.1016/j.desal.2023.116888.

[51] Dai C. et al., 2024, Hydrolyzed PAN Nanofibers for Nanofiltration Membranes, Journal of Membrane Science, 693,122398, https://doi.org/10.1016/j.memsci.2023.122398.

[52] Liang B. et al., 2014, Hydrophilic Pervaporation Composite Membranes for Desalination, Desalination, 347,199-206.

[53] Liang B. et al., 2015, Graphene Oxide/PAN Composite Membranes for Desalination, Journal of Materials Chemistry A, 3,5140-5147.

[54] Su M. et al., 2010, Dual-Layer Hollow Fiber Membranes in Membrane Distillation, Journal of Membrane Science, 364,278-289.

[55] Edwie F. et al., 2012, Effects of Additives on PVDF Hollow Fiber Membranes, Chemical Engineering Science, 68,567-578.

[56] Liu B. et al., 2022, Polyvinyl Alcohol Water-Resistant Film Materials, Membranes, 12,3,347.

[57] Nagandran S. et al., 2020, Modification of Polymeric Membranes Using Organic Macromolecules, Symmetry, 12,2,239.

[58] Sapalidis A.A., 2020, Porous Polyvinyl Alcohol Membranes, Symmetry, 12,6,960.

[59] Filimon A. et al., 2025, Polyvinyl Alcohol-Based Membranes, Polymers, 17,8,1016.

[60] Nagarkar R., dan Patel J., 2019, Polyvinyl Alcohol: A Comprehensive Study, Acta Scientific Pharmaceutical Sciences, 3,4,34-44.

[61] Restrepo I. et al., 2018, Effect of Molecular Weight and Hydrolysis Degree of PVA, Polímeros, 28,169-177.

[62] Saad M.A. et al., 2025, Sodium Alginate/PVA Hydrogel for Desalination, Scientific Reports, https://doi.org/10.1038/s41598-024-58533-6.

[63] Liu Q. et al., 2026, Chitosan/PVA Aerogel for Solar Desalination, Colloids and Surfaces A, https://doi.org/10.1016/j.colsurfa.2026.140341.

[64] da Silva D.A.R.O. et al., 2021, Pretreatments for Seawater Desalination Using PVA Membrane, Journal of Environmental Chemical Engineering, https://doi.org/10.1016/j.jece.2021.106327.

[65] Selim M.A. et al., 2020, Pervaporative Desalination Using PVA Membranes, Chemical Engineering Research and Design, 155,229-238, https://doi.org/10.1016/j.cherd.2020.01.015.

[66] El-Gendi A. et al., 2017, PVC/Cellulose Acetate Blend Membranes for Desalination, Journal of Molecular Structure, 1146,14-22.

[67] Zachariah S., dan Liu Y.L., 2021, Surface Engineering of PVA Membranes for Desalination, Journal of Membrane Science, https://doi.org/10.1016/j.memsci.2021.119670.

[68] Yang G. et al., 2019, Enhanced Desalination Performance of PVA Membranes, Journal of Membrane Science, 579,40-51, https://doi.org/10.1016/j.memsci.2019.02.034.

[69] Chaudhri S.G. et al., 2018, PVA-Silica Pervaporation Membrane, Journal of Applied Polymer Science, https://doi.org/10.1002/app.45718.

[70] Li Q. et al., 2018, High Performance Pervaporation Desalination Membrane, Industrial & Engineering Chemistry Research, 57,11178-11185.

[71] Zhang R. et al., 2019, Cross-Linked PVA Composite Membrane for Desalination, Environmental Technology, 40,312-320.

[72] da Silva D.A.R.O. et al., 2020, Green Silica/PVA Membrane for Desalination, Separation and Purification Technology, 247,116852.

[73] Meng J. et al., 2021, Thin-Film Composite Membranes for Desalination, Desalination, 512,115128, https://doi.org/10.1016/j.desal.2021.115128.

[74] Zhao P. et al., 2020, Chemical Resistant Pervaporation Membranes, Journal of Membrane Science, 611,118367.

[75] Li L. et al., 2017, Composite PVA/PVDF Membrane for Brine Desalination, Desalination, 422,49-58.

[76] Zhao X. et al., 2021, Cellulose Acetate/Activated Carbon Composite Membrane, Journal of Chemical Technology and Biotechnology, 96,672-679.

[77] Seong J.G. et al., 2021, Microporous Polymers for Gas Transport, Science Advances, 7,eabi9062.

[78] Zhao X. et al., 2019, Cellulose Acetate/Activated Carbon Membrane for Dye Adsorption, Journal of Macromolecular Science Part B, 58,909-920.

[79] Fan H., dan Elimelech M., 2025, Solvent Transport in Membrane Pores, Environmental Science & Technology, 59,17922-17931.